A Single Lens Micro-Angle Sensor

Yusuke Saito[1,#], **Wei Gao**[1] and **Satoshi Kiyono**[1]

1 Nanosystems Engineering Lab, Department of Nanomechanics, Tohoku University
Corresponding Author / E-mail: saito@nano.mech.tohoku.ac.jp; TEL: +81-22-795-6953; FAX: +81-22-795-6953

Angle sensors based on the principle of autocollimation, which are usually called autocollimators, can accurately measure small tilt angles of a light-reflecting flat surface. This paper describes a prototype micro-angle sensor that is based on the laser autocollimation technique. The new angle sensor is compact and consists of a laser diode as the light source and a quadrant photodiode as a position-sensing device. Because of its concise design, the micro-angle sensor facilitates dynamic measurements of the angular error motions of a precision stage without influencing the original dynamic properties of the stage. This is because the sensor only requires a small extra target mirror to be mounted on the stage. The sensitivity of the angle detection is independent of the focal length of the objective lens; therefore, an objective lens with a relatively short focal length is employed to reduce the size of the device. The micro-angle sensor uses a single lens for the both the laser collimation and focusing, which distinguishes it from the conventional laser autocollimation method that has separate collimate and objective lenses. The new micro-angle sensor has dimensions of 15. 1 × 22.0 × 14.0 mm and its resolution is better than 0.1 arc-second. The optical design and performance of this micro-angle sensor were verified by experimental results.

1. Introduction

Geometric parameters, such as angles and lengths, usually serve as benchmarks for precise motion control. Recently, ultraprecision stages have become widely used in precision processing machines, semiconductor manufacturing, inspection devices, and other precision measuring systems. The measurement of stage movement errors is essential in evaluating the performance of these machines [1,2].

Stage movement errors can be expressed as a position error and a translational motion (straightness) error along the direction of motion. The former error can be measured using a laser interferometer or linear encoder, while the latter error is usually measured based on a straightedge. [3] Figure 1 shows the angle errors of a stage during one-dimensional motion. The difference between the interferometers that are preset on the stage must be read to provide posture angle control. However, this increases the complexity of the measurement system since the number of position-detecting sensors must equal the dimensions of the angle motions that need to be measured. High performance angle sensors are therefore required. These sensors must be highly sensitive with fast response times, and must be capable of noncontact measurements.

Autocollimators, which use the principle of autocollimation, are commonly used for minute angle measurements. When the optical beam that contains the angle information from the reflecting surface, usually a mirror, is focused on the focal plane of the objective lens, the amount of displacement can be detected from the proportion of the light spot that falls on given cells by using an optical positional detective element. [4-9] The objective lens plays the role of an angle

magnifier: the longer the focal length, the greater the magnification of the angle. Since an autocollimator uses a charge-coupled device (CCD) as the photoelectric element, the frequency-measuring capability is usually on the order of tens of hertz. Thus, it cannot be used for dynamic measurements. Furthermore, the sensitivity of a CCD is low so that a relatively large lens with a focal length of hundreds of millimeters is required to yield highly sensitive angle detections., which makes the autocollimator bulky, expensive, and difficult to integrate with other precision systems. [10,11]

A laser autocollimation system is a combination of a thin laser beam with a photodiode detector. Since they are highly sensitive, have fast measuring speeds, and provide more horizontal resolution than conventional autocollimators, they have been widely applied to ultraprecision shape measurements. [12-16] It is also possible to use an objective lens with a short focal length without reducing the sensitivity of the system, which facilitates miniaturization of the angle sensor. [17-20]

The aim of this study was to develop a compact but highly sensitive angle sensor based on the principle of laser autocollimation. The target specifications were as follows: an angle resolution of 0.1 arc-second (1 kHz in frequency band region), a measurement range of 50 seconds, and a system bulk volume of less than 15 mm. [3]

2. Principle of Angle Detection

2.1 Laser autocollimation method

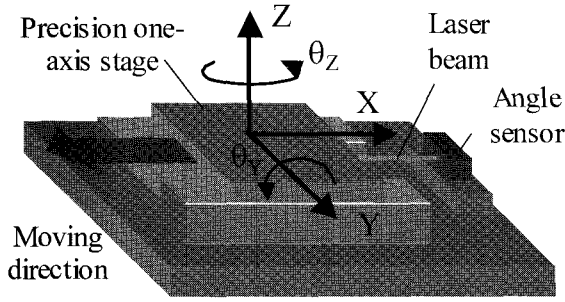Figure 2(a) shows the principle of a laser autocollimation system

Fig. 1 Angle errors of a stage during one-dimensional motion

in geometric optics. A relationship exists between the angle $\Delta\theta_Z$ and the focal length f:

$$\Delta\theta_Z = \arctan\left(\frac{d_Y}{f}\right) \doteq \frac{d_Y}{f}. \tag{1}$$

It is possible to calculate the change of the tilt angle of the sample just by detecting the change of the spot position on the photodetector. Figure 2(b) shows the changes in the beam spot position for angles of $\Delta\theta_Z$ and $\Delta\theta_Y$.

2.2 Sensitivity of the angle sensor

A quadrant photodiode (QPD) was employed in the new angle sensor due to its two-dimensional position-detecting capability as well as its high sensitivity compared to other position detectors. Figure 3 shows a schematic view of the spot on the QPD cells when the angle has changed. Assuming the laser beam has a Gaussian intensity distribution, the spot size on the QPD can be obtained from [21]

$$w_{Y0} = \frac{1.22 f\lambda}{D_Y}, \quad w_{Z0} = \frac{1.22 f\lambda}{D_Z}, \tag{2}$$

where D_Y and D_Z are the beam diameters, w_{Y0} and w_{Z0} give the spot diameters in the Y and Z directions, f is the focal length of the objective lens, and λ is the wavelength. Assuming that no gap exists between the photodiode (PD) cells, the intensity distribution of the optical spot and the current conversion sensitivity will be uniform in each cell. The output of the QPDs (Y_{out}, Z_{out}) can be expressed as
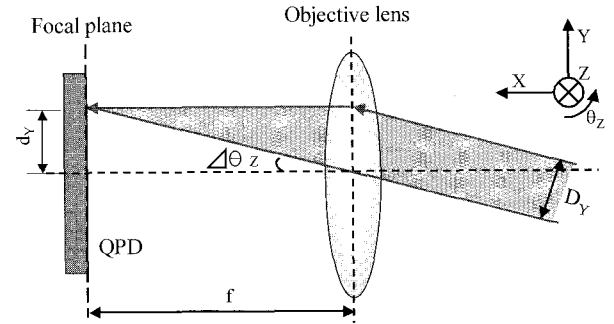
$$Y_{out} = \frac{(I_A + I_B) - (I_C + I_D)}{I_A + I_B + I_C + I_D} \times 100\%$$

, and

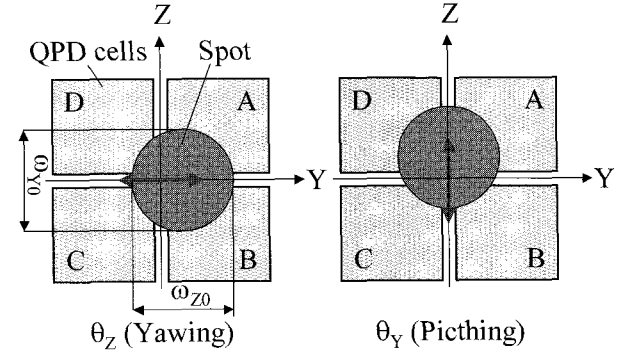$$Z_{out} = \frac{(I_A + I_D) - (I_B + I_D)}{I_A + I_B + I_C + I_D} \times 100\%, \tag{3}$$

where I_A, I_B, I_C, and I_D are the photocurrents of each QPD cell, which are proportional to the light spot areas of the corresponding cells. Dividing by the total output value compensates for the change in the intensity of the incident light and the influences of the gaps between the PD cells. When the incident beam has inclination of $\Delta\theta_Z$, the spot diameter displacement w_{Y0}, corresponding to the position d_Y, occurs on the focal plane (see Eq. (1)). The difference between incident spot areas of cells A, B, C, and D can be approximately expressed by $4w_{Y0}\,d_Y$. Since the entire area of the optical spot is $\pi w_{Y0} w_{Z0}$, Eq. (3) can be rewritten as

$$Y_{out} = \frac{4w_{Z0} d_Y}{\pi w_{Y0} w_{Z0}} \times 100\% = \frac{4 d_Y}{\pi w_{Y0}} \times 100\% \approx \frac{D_Y \Delta\theta_Z}{\lambda} \times 100\%$$

$$Z_{out} \approx \frac{D_Z \Delta\theta_Y}{\lambda} \times 100\%. \tag{4}$$

(a) Schematic of θ_Z angle detection

θ_Z (Yawing) θ_Y (Picthing)

(b) Behavior of the beam spot on the QPD cells

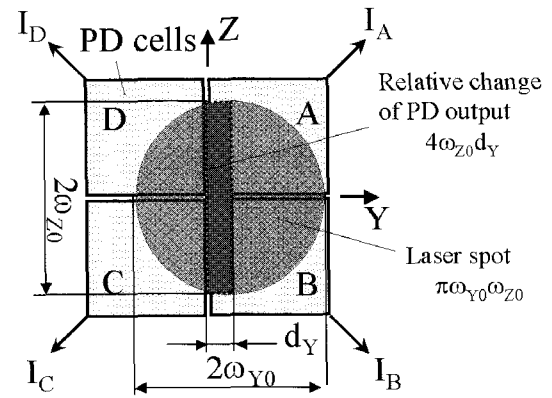Fig. 2 Principle of angle detection by laser autocollimation

Fig. 3 Behavior of the beam spot on the QPD cells

The sensitivity of the angle sensor S_Y and S_Z can then be approximated as the percentage of the sensor output to the incident angle ($\Delta\theta_Y$, $\Delta\theta_Z$)

$$S_Y = \frac{Y_{out}}{\Delta\theta_Z} = \frac{D_Y}{\lambda} \times 100\%, \quad S_Z = \frac{D_Z}{\lambda} \times 100\% \tag{5}$$

The sensitivity only depends on the incident beam diameter and wavelength, and has no relation to the focal length of the objective lens. Therefore, it is possible to develop a highly sensitive and compact angle sensor by using an objective lens with a relative short focal length.

3. Simulations

3.1 Output characteristics of the angle sensor

Figure 4(a) shows the simulated output of the angle sensor Y_{out} for different focal lengths of 8, 40, and 80 mm. The intensity of the incident beam was 1 mW, and the beam was assumed to be circular with a half bandwidth $D_Z/2$ Gaussian distribution. The sensitivity was defined as the ratio of the output angle from the sensor over the input angle. The sensitivity of the 8-mm focal length was greater than that of the 40- and 80-mm focal lengths, which indicates that the sensitivity had no direct relation to the focal length of the objective lens.

In the previous section, the gaps between the QPD cells were assumed to be zero. However, the simulations included a 10-μm gap. Figure 4(b) shows that the output characteristics of the sensor were greatly influenced by the QPD gap (dead zone) between the PD elements. The sensitivity increased with the size of the gap. When the incident beam had a Gaussian intensity, the majority of the beam energy was concentrated on the center part of the beam. If the spot center happened to be on the QPD gap, the output signals of each PD cell decreased greatly. From Eq. (3), the sensitivity of the angle sensor then increased dramatically since the beam energy from all the PD cells became the denominator in the final results. However, enlarging the QPD gap may decrease the signal/noise ratio of the sensor signal output.

3.2 Applying an offset to the QPD

Although the dimensions of the senor can be minimized by using an objective lens with a short focal length, a restriction still exists for choosing the minimum focal length since the laser spot diameter must be larger than the gaps between the PD cells. An offset technique, schematically shown in Fig. 5(a), was employed to make the senor more compact. The beam diameter along the X-axis can be expressed as [22]

$$w(\Delta x) = w_0 \left[1 + \left(\frac{\lambda \Delta x}{\pi w_0^2} \right)^2 \right]^{\frac{1}{2}}, \tag{6}$$

where ω_0 is the spot radius on the focal plane and Δx is the offset beyond the focal position. The simulated results (see Fig. 5(b)) show that the resolution and measuring range of the angle sensor were dramatically enhanced when an offset was used. The focal length was 8 mm, and the offset was set to 0, 100, or 400 μm. The gap size was 10 μm; the other conditions are listed in Table 1.

3.3 Interference error between the two-axial outputs

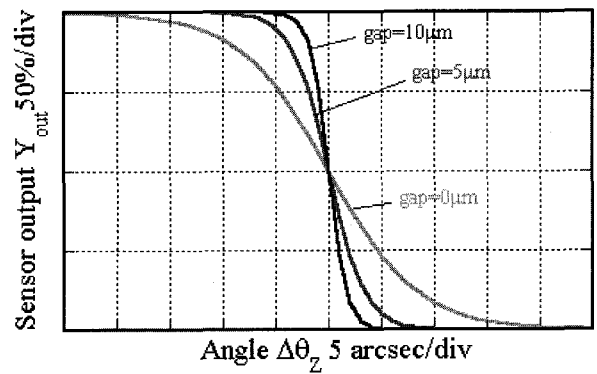The micro-angle sensor can theoretically detect pitching and

Table 1 Simulated conditions

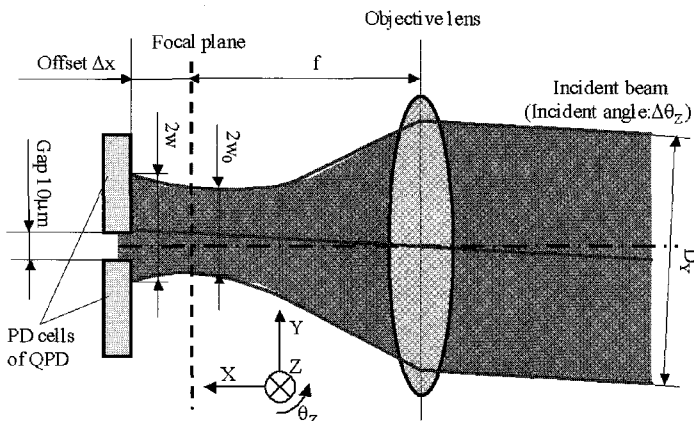|	
Focal length of lens	f = 8, 40, and 80 mm
QPD gap size and active area	Gap size: 0, 5, and 10 μm Active area: 1.2×0.6 mm^2
Condition of the incident beam (Gaussian beam profile)	Dz: $\phi = 1$ mm λ: 635 nm Output intensity: 1 mW
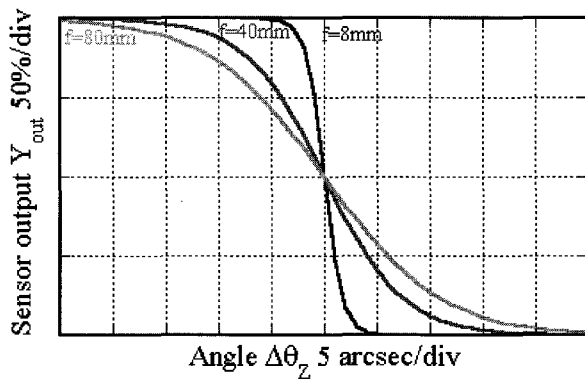
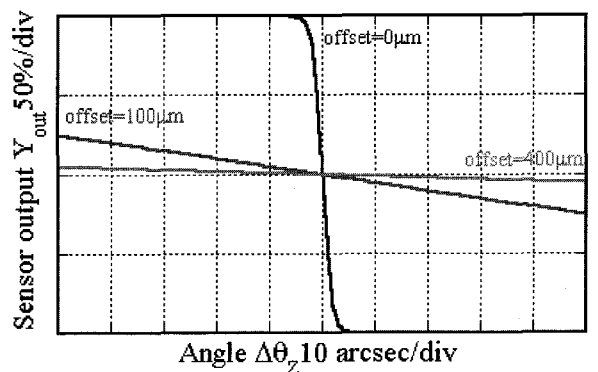(a) Effect of the focal length

(b) Effect of the QPD gap

Fig. 4 Simulated angle sensor results

(a) Applying an offset to the QPD

(b) Effect of the QPD position

Fig. 5 Simulated results with a QPD offset

yawing simultaneously by using a QPD as the detector. This was confirmed by another simulation, in which the offset was set to 100 μm while the other conditions remained the same as those listed in Table 1. The θ_Y directional angle was changed from 0 to 80 arc-seconds with a step of 20 arc-seconds. The Y_{out}-directional outputs of the angle sensor at different θ_Y angles, shown in Fig. 6, were identical, indicating the two-axis measuring capability of the senor.
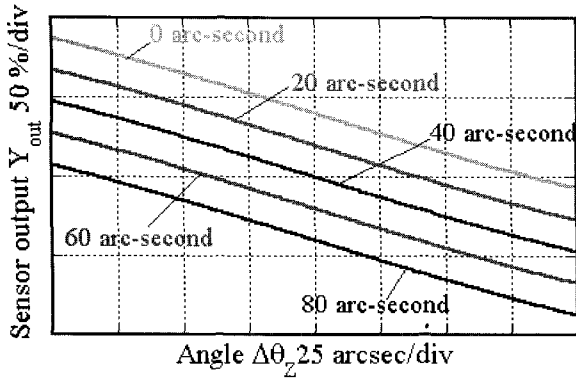

Fig. 6 Simulation outputs (interference of the output)

4. Experiments

4.1 Design of the micro-angle sensor with a single lens

Figure 7(a) shows a schematic view of a conventional angle sensor with a laser diode (LD) light source. A laser beam with P polarization was collimated to a parallel beam and passed through a polarized beam splitter (PBS). Then the polarization of the laser beam was converted from P to circular polarization by a quarter-wave plate (λ/4 plate). The reflected beam returned back to the λ/4 plate and became an S polarized beam after passing through the plate. The beam was then bent at the PBS and entered the autocollimation unit consisting of an objective lens and a sensitive high-speed QPD photodetector that was preset at the focal plane. The combination of the PBS and the quarter-wave plate functioned as an optical isolator to prevent the light beam from returning to the laser diode, thus making the LD output stable.

Figure 7(b) shows the optical layout of the new micro-angle senor (MAS). The MAS only used a single lens that had the dual purposes of collimating and focusing the light. This configuration minimized the number of components and made the MAS more compact. The assembly was also simplified since the displaying LD, PBS, and lens were on a single straight line. The QPD was set up with an offset beyond the focus position of the objective lens along the axis to obtain sufficient output voltage.

4.2 Change in the focal length of the lens

The LD light source beam in the MAS had extension angles in both the horizontal and vertical directions, which caused the laser to reflect on the boundary sides of the PBS and quarter-wave plate. This can change the focal length and must be defined in advance.[23] Figure 8(a) shows a geometrical optics model of the laser reflection, where θ_1 is the extension angle of the LD; θ_2 and θ_5 are the reflecting angles on each boundary edges; l_5 is the difference between the effective focal length (EFL) and back focal length (BFL); r is the curvature of the lens; and n_{air}, n_{PBS}, $n_{1/4}$, and n_{lens} are the reflective index of each material. The change in the focal length l_1 can be expressed using Snell's law as

$$l_1 = \frac{1}{\tan\theta_1}\left(r\sin\theta_5 - (l_2\tan\theta_2 + l_3\tan\theta_3 + l_4\tan\theta_4)\right) \qquad (7)$$

The focal length of the lens required for the 8-mm MAS was determined to be 9.6 mm using this equation.

The finalized MAS, with dimensions of 15.1 × 22.0 × 14.0 mm and a weight of 50 g, is shown in Fig. 8(b). A 3-mW intensity laser diode adjusted to approximately 1 mW was used as the light source. It was collimated to a parallel beam with an approximate diameter of 2.7 mm.
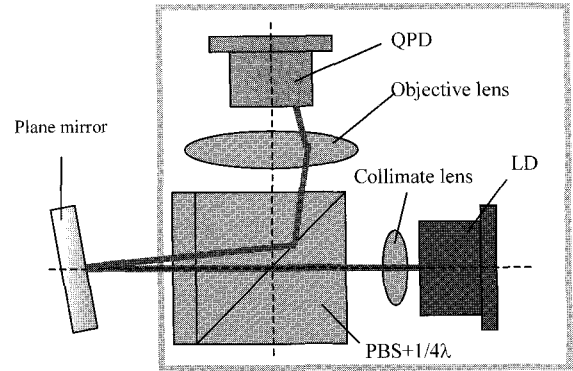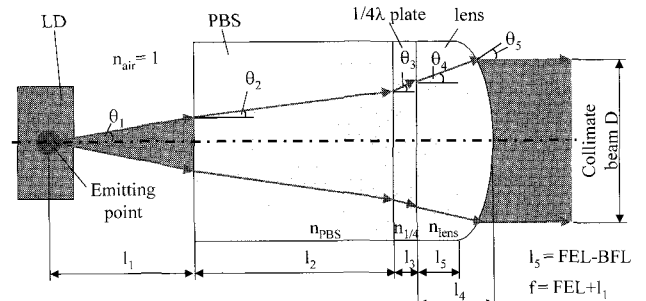

(a) Conventional angle sensor (with two lenses)
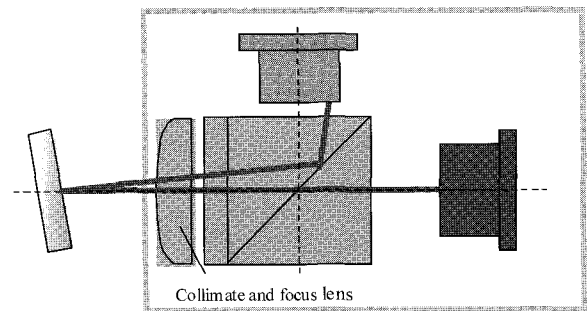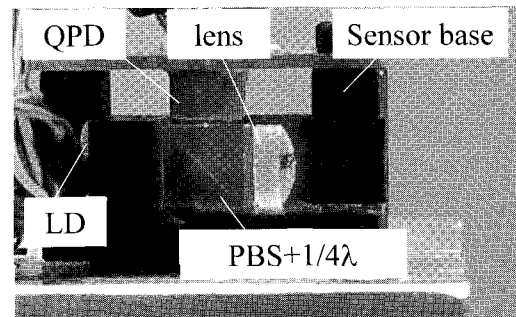

(b) Micro-angle sensor (with a single lens)

Fig. 7 Optical layouts of the angle sensors

(a) Geometrical optics model of the laser reflection

(b) Photograph of the MAS

Fig. 8 Structure of the micro-angle sensor with a single lens

4.3 Experimental setup

Figure 9 shows a schematic view of the experimental setup. It consisted of a PZT-driven tilt stage on which two mirrors were mounted to generate the two-axis tilt motions θ_Y and θ_Z. The performance of the MAS was evaluated by measuring the tilt angles

of the stage simultaneously with a commercial autocollimator. The commercial autocollimator had a resolution of 0.1 arc-second, an accuracy of 0.2 arc-second, and a measuring range of 600 arc-seconds.
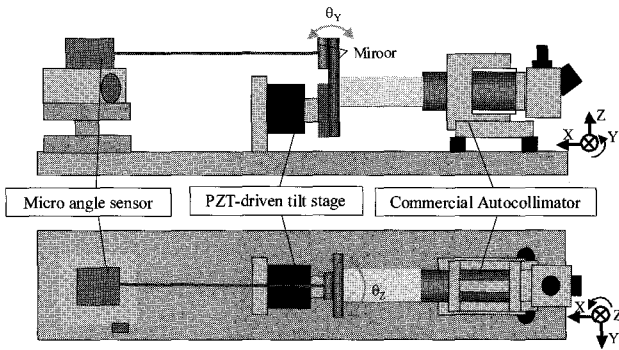

Fig. 9 Setup of the evaluation experiments

4.4 Experimental results

Figure 10 shows the output obtained from the two measuring devices when a sinusoidal signal with a frequency of 0.1 Hz and an amplitude of ±50 arc-seconds was applied to drive the PZT tilt stage. The horizontal axis in the figure gives the output of the autocollimator and the vertical axis gives the output of the MAS. The two outputs had a linear relationship. However, some data deviations were apparent in the θ_Y (Fig. 10(a)) and θ_Z (Fig. 10(b)) results; thus advance adjustments were necessary.

Figure 11 shows the results of the resolution test, for which a sinusoidal signal with a frequency of 0.1 Hz and amplitude of 0.3 arc-second was applied. The resolution of the MAS was greater than that of the commercial autocollimator.

Figure 12 illustrates the stability of the MAS. These results had a noise width of approximately 0.1 arc-second in both the θ_Y and θ_Z signals; therefore, the MAS had a measurement capability up to 0.1 arc-second.

5. Conclusions

The following conclusions were drawn from this study.
(1) A micro-angle sensor with a single lens was developed based on the laser autocollimation technique. The sensor was compact, with dimensions of 15.1 × 22.0 × 14.0 mm and a weight of 50 g.
(2) The angle detection sensitivity of the sensor only depended on the diameter (D_Y, D_Z) and wavelength (λ) of the incidence laser beam and was not related to the focal length of the objective lens.
(3) The resolution and measuring range of the sensor could be dramatically enhanced by applying an offset to the QPD.
(4) The sensor had an angle resolution of 0.1 arc-second (15 kHz in frequency band range) and its measurement capability was comparable to that of a commercial autocollimator.
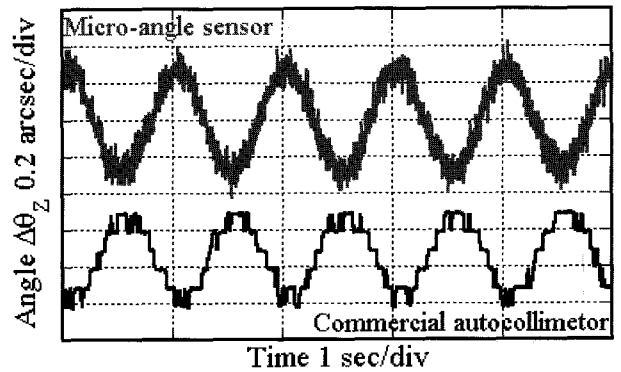
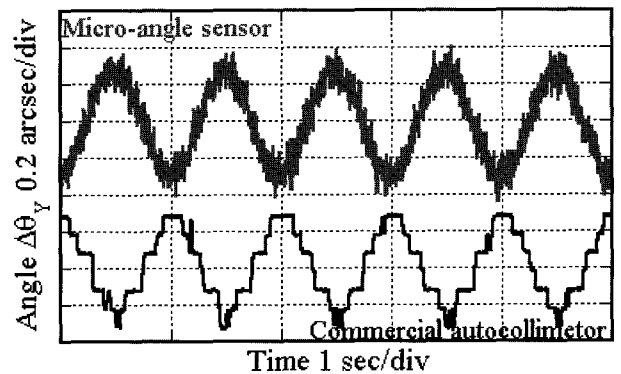## ACKNOWLEDGEMENT
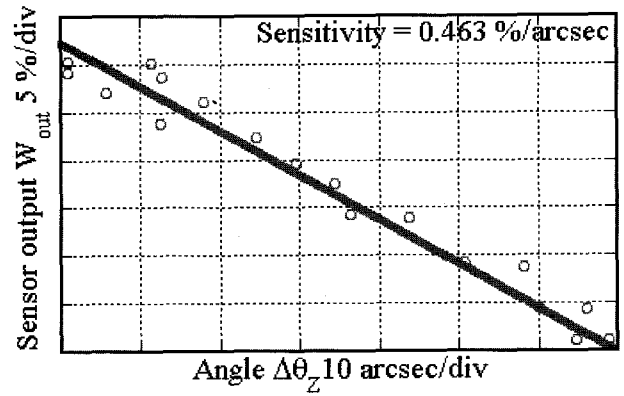
(a) Sensor Y_{out} output
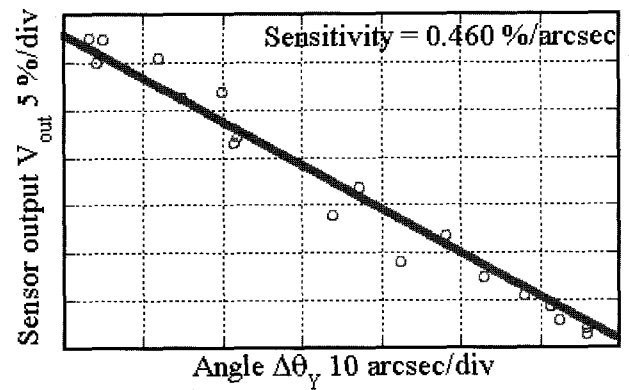
(b) Sensor Z_{out} output

Fig. 10 Output of the micro-angle sensor

(a) $\Delta\theta_Z$ angle direction

(b) $\Delta\theta_Y$ angle direction

Fig. 11 Resolution test results for the micro-angle sensor and the autocollimator
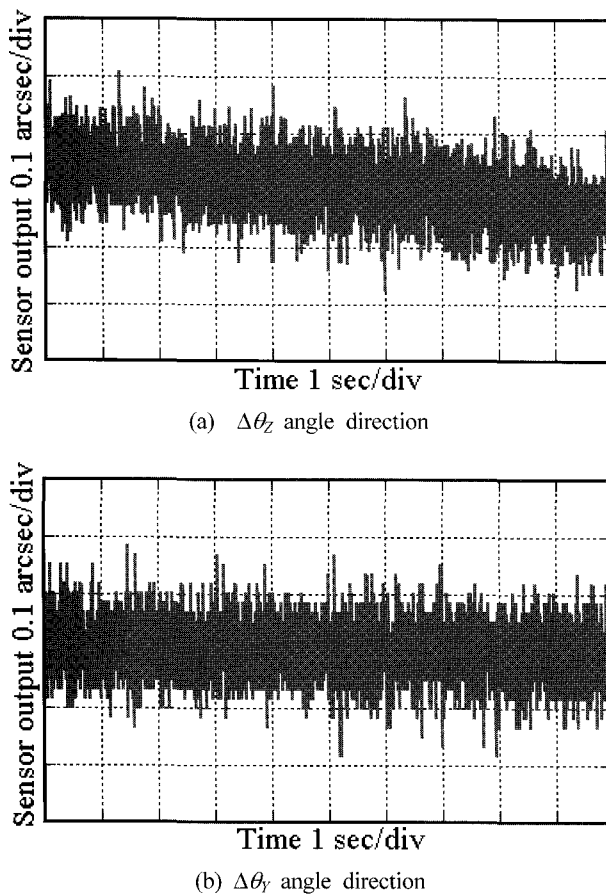
(a) $\Delta\theta_Z$ angle direction

(b) $\Delta\theta_Y$ angle direction

Fig. 12 Stability of the micro-angle sensor

REFERENCES

1. Moore, W. R., "Foundations of Mechanical Accuracy," The Moore Special Tool Company, 1970.

2. Gao, W., Ohnuma, T., Satoh, H., Shimizu, H. and Kiyono, S., "A precision angle sensor using a multi-cell photodiode array," Annals of the CIRP, Vol.53, No.1, pp.425–428, 2004.

3. Farago, F. T. and Curtis, M. A., "Handbook of Dimensional Measurement," Industrial Press, 1994.

4. Estler, W. T. and Queen, Y. H. "Angle metrology of dispersion prisms," Annals of the CIRP, Vol.49, No.1, pp. 415–418, 2000.

5. Yanadayan, T., Akgoz, S. A. and Hitjema, H., "A novel technique for calibration of polygon angles with non-integer subdivision of indexing table," Precision Engineering, Vol.26, No.4, pp.412–424, 2002.

6. Gackeler, R. D., Just, A., Probst, R. and Weingartner, I., "Sub-nm to topography measurement using high-accuracy autocollimations," Technisches Messen, Vol.69, No.12, pp.535–541, 2002.

7. Gao, W., Tano, M., Sato, S. and Kiyono, S., "On-machine measurement of cylindrical surface with sinusoidal micro-structures by an optical slope sensor," Precision Engineering, Vol.30, pp.274–279, 2006.

8. Kiyono, S., Cai, P. and Gao, W., "An angle-based detection method for precision machines," JSME International Journal, Vol.42, No.1, pp. 44–48, 1999.

9. Gao, W., Dejima, S. and Kiyono, S., "A dual-mode surface encoder for position measurement," Sens Actuators A, Vol.117, No.1, pp.95–102, 2005.

10. http://www.keyence.co.jp/

11. http://www.surugaost.jp/

12. Ennos, A. E. and Virdee, M. S., "High accuracy profile measurement of quasi-conical mirror surfaces by laser autocollimation," Precision Engineering, Vol.4, No.1 pp.5–8, 1982.

13. Gao, W. and Kiyono, S., "Development of an optical probe for profile measurement of mirror surfaces," Optical Engineering, Vol.36, No.12, pp.3360–3366, 1997.

14. Kiyono, S., Asakawa, Y., Inamoto, M. and Kamada, O., "A differential laser autocollimation probe for on-machine measurement," Precision Engineering, Vol.15, No.2 pp.68–76, 1993.

15. Gao, W., Kiyono, S. and Satoh, E., "Precision measurement of multi-degree-of-freedom spindle errors using two-dimensional slope sensors," Annals of the CIRP, Vol.51, No.1, pp.447–450, 2002.

16. Gao, W., Dejima, S., Shimizu, Y. and Kiyono, S., "Precision measurement of two axis positions and tilt motions using a surface encoder," Annals of the CIRP, Vol.52, No.1 pp.435–438, 2003.

17. Gao, W., Huang, P. S., Yamada, T. and Kiyono, S., "A compact and sensitive two-dimensional angle probe for flatness measurement of large silicon wafers," Precision Engineering, Vol.26, No.4, pp.396–404, 2002.

18. Virdee, M. S., "Nanometrology of optical flats by laser autocollimation," Surface Topography, Vol.1, pp.415–425, 1988.

19. Gao, W., Kiyono, S. and Nomura, T., "A new multiprobe method of roundness measurements," Precision Engineering, Vol.19, No.1 pp. 55–64, 1996.

20. Weingartner, I., Schulz, M. and Elster, C., "Novel scanning technique for ultra-precise measurement of topography," SPIE, Vol.3782, pp.306–317, 1999.

21. Murata, K., "Optics," Saiensu-Sha, 1979.

22. O'Shea, D. C., "Elements of Modern Optical Design," John Wiley & Sons, 1985.

23. http://www.edmund.co.jp/